EFFECT OF STRENGTH MISMATCH AND DYNAMIC LOADING ON THE DUCTILE CRACK INITIATION FROM NOTCH ROOT

by Gyu-Baek AN*, Satoshi YOSHIDA, Mitsuru OHATA and Masao TOYODA

Graduate School of Engineering Osaka University,
2-1, Yamada-oka Suita, Osaka 565-0871, Japan, angb@mech.eng.himeji-tech.ac.jp

ABSTRACT

It has been well known that ductile fracture of steels is accelerated by triaxial stresses. The characteristics of ductile crack initiation in steels are evaluated quantitatively using two-parameters criterion based on equivalent plastic strain and stress triaxiality. It has been demonstrated by authors using round-bar specimens with circumferential notch in single tension that the critical strain to initiate ductile crack from specimen center depends considerably on stress triaxiality, but surface cracking of notch root is in accordance with constant strain condition. In order to evaluate the stress/strain state in the specimens, especially under dynamic loading, a thermal, elastic-plastic, dynamic finite element (FE)analysis considering the temperature rise due to plastic deformation has been carried out.

This study provides the fundamental clarification of the effect of strength mismatching, which can elevate plastic constraint due to heterogeneous plastic straining, loading mode and loading rate on critical condition to initiate ductile crack from notch root using equivalent plastic strain and stress triaxiality based on the two-parameter criterion obtained on homogeneous specimens under static tension.The critical condition to initiate ductile crack from notch root for strength mismatched bend specimens under both static and dynamic loading would be almost the same as that for homogeneous tensile specimens with circumferential sharp notch under static loading.

KEYWORDS

Ductile crack initiation, dynamic loading, strength mis-match, stress-triaxiality; equivalent plastic strain.

1. Introduction

The weld joint often has characteristics of the strength mismatch in general steel structures. Plastic constraint and strain rate are considered to have complicated effects on the initiation behavior of ductile crack as well as deformation behavior of materials in the strength mismatching part under the dynamic loading condition such as earthquakes [1, 2]. The important characteristics of this earthquake were the occurrence of brittle failures of steel structures under high speed ground motion (104 kine (cm/s)) and significant ground displacement (27 cm) [1-4].

Therefore, it is important to elucidate initiation condition and dominate factor of ductile crack and to establish a general criterion to conduct safety assessment in the steel structure with strength mismatch under dynamic loading. In order to discuss possibilities of brittle fractures after large scale deformation in earthquakes, it is important to clarify ductile fracture initiation and propagation. Furthermore, when considering the behavior of welded joints under seismic loading, the effect of strength mismatch and dynamic loading on the fracture behavior of the connection zones has to be studied. In the present paper, attention was given to the critical evaluation of ductile fracture initiation in the connection zones of steel framed structures under seismic loading, taking into account the combined effects of strength mismatch and dynamic loading.

An estimation of ductile crack initiation, however, would have a difficulty in the case that the ductile cracking would occur from the surface of geometrical stress/strain concentration region with strength mismatch, which elevates the plastic constraint. To apply the initiation condition of ductile crack using two-parameter to the critical assessment of ductile crack initiation in actual structures as a general criterion, it remains to the subject to clarify the initiation condition of ductile crack from the surface of steel structures with strength mismatch near the geometrical discontinuity part like welded joint [5, 6].

This study provides the fundamental clarification of the effect of strength mismatch, which can elevate plastic constraint due to heterogeneous plastic straining, loading mode and loading rate on critical condition to initiate ductile crack from notch root using two-parameter. The behavior of ductile crack initiation from pre-notch root and effect of strength mismatch were investigated by bending test using charpy type specimens. Moreover, in order to evaluate the ductile crack initiation behavior in the specimen under static and dynamic loading, thermal, elastic-plastic, dynamic FE-analysis considering the temperature rise due to plastic deformation has been carried out. Finally, it is shown that the condition for ductile crack initiation using the two parameters equivalent plastic strain and stress triaxiality is a transferable criterion for ductile crack initiation from surface of pre-notch root.

2. Experimental Method

The weld joint with strength mismatch was made by electro gas welding using welding wire for 50kgf class steel

and HT80 steel of plate thickness 22mm as a base metal. A welding condition and chemical composition of the base metal are shown in Table 1 and 2, respectively. A vickers hardness distribution of a near of welded joint in plate thickness central part are shown in Fig. 1. The nominal stress-nominal strain curves obtained from tensile tests of smooth round-bar for homogeneous specimens are shown in Fig. 2. The mechanical properties of the weld metal and base metal are given in Table 3. This welded joint is a strength mismatched joint with strength ratio of yield stress ($Sr(Y)$) and tensile strength ($Sr(T)$) is about 1.7 and 1.3, respectively.

Table 1 Welding condition for EGW.

Electro Gas Arc Welding (EGW)		
Wire	Weld heat input	Shield gas
1.6mmφ Flux wire	142~153 (kJ/cm)	100%CO_2

Table 2 Chemical composition of base metal (HT80 steel) used.

Steel	C	Si	Mn	P	S	Cu	Ni	Cr	Mo	V	Ti	Nb	Al	B	C_{eq}	P_{cm}
HT80	0.10	0.26	0.85	0.004	0.002	0.23	1.16	0.49	0.47	0.037	0.016	0.011	0.046	0.0012	0.50	0.25

Table 3 Mechanical properties of weld metal and base metal used.

Material	s_Y (MPa)	s_T (MPa)	YR	Sr(Y)	Sr(T)	e_T(%)	EL. (%)
Base metal (BM)	848	887	96	1.67	1.30	6.0	30.8
Weld metal (WM)	509	684	74			11.4	32.0

s_Y : 0.2% proof stress, s_T : Tensile strength, YR : Yield to tensile ratio s_Y/s_T,
Sr(Y) : s_Y^{BM}/s_Y^{WM}, Sr(T) : s_T^{BM}/s_T^{WM}, e_T : Uniform elongation,
El. : Elongation (G.L.=12mm, Dia.=6mm)

In order to assess the criterion for ductile cracking of weld metal, round bar tensile specimens with and without circumferential notch in weld metal presented in Fig. 3 were used. Round bar tension specimens with diameter of 10mm were used. The radius of curvature of the notch root R=0.1mm specimen(T-R0.1) was employed by author's experiment result[7, 8, 9] which expected the ductile crack initiation of surface of pre-notch. In addition to smooth round bar tensile specimen with a diameter of 6mm, in order to investigate of ductile crack initiation from center two types of circumferentially notched tensile specimens with different radius of curvature R of the notch root-T-R1 and T-R2 denotes the specimens with radius of curvature R=1 and 2mm respectively-which have the same diameter of 6mm in minimum cross section in all specimen were employed. The characteristic of ductile crack initiation from surface of pre-notch root and effect of strength mismatch were investigated using a charpy type bend specimen with sharp V type notch, comparison with characteristics of ductile crack initiation for homogeneous specimen (weld metal). Figure 4 presents the configuration of 2 kinds of three-point bend test specimens used. One is a strength mismatch specimen in which a notch tip is located in fusion line of welded joint and another is a homogeneous specimen with a notch in the center of weld

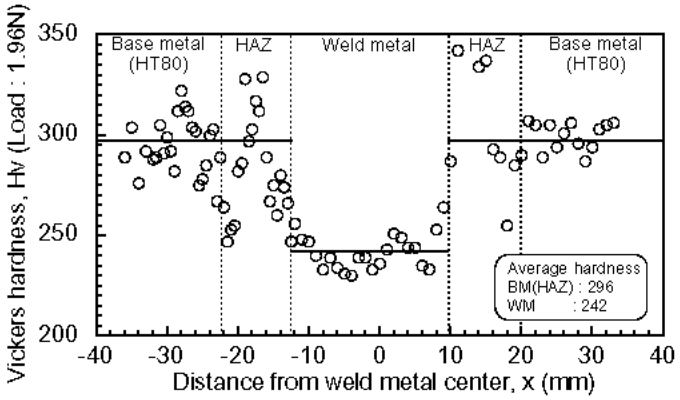

Fig. 1 Vickers hardness distribution of welded joint.

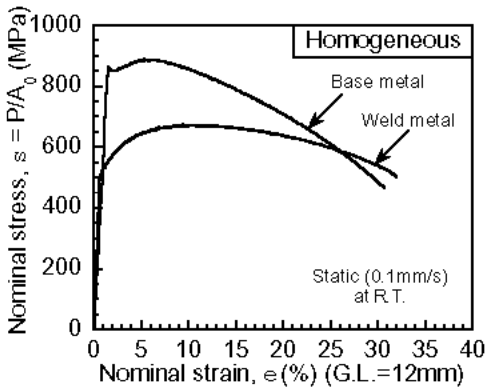

Fig. 2 Nominal stress, s - nominal strain, $e$curves for base metal and weld metal under static loading, 0.1mm/s.

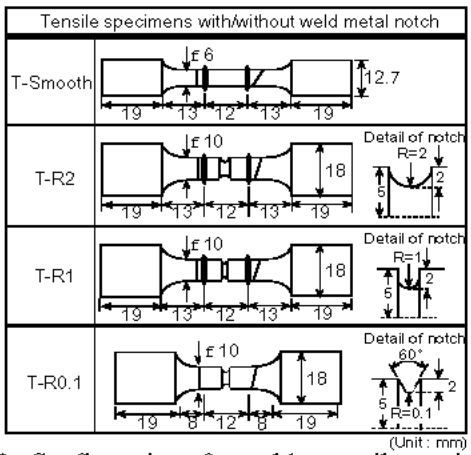

Fig. 3 Configuration of round-bar tensile specimens with /without weld metal notch.

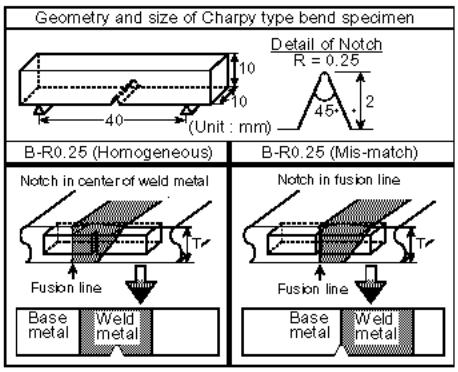

Fig. 4 Geometry and size of 3-point bend specimens.

metal. These specimens have through-thickness notch with a radius of curvature of notch root R=0.25mm. Ductile crack initiation behaviors were observed center and surface of pre-notch of specimens by carried out unloading tests at a particular loading levels-cross section and ductile cracking surface of the specimens which were fractured in brittle manner after unloading and cutting at mid-thickness.

3. Criterion for Ductile Crack Initiation Obtained by Small Scale Tensile Specimens for Homogeneous Material

A ductile crack initiation behavior was observed using round bar specimens with and without circumferential notch in weld metal under static loading. Critical condition for ductile crack initiation of weld metal was addressed using two-parameter which are equivalent plastic strain and stress triaxiality obtained by FE-analysis.

3.1 Ductile crack initiation behavior of homegeneous materials

For all specimens shown in Fig. 3, tensile tests were carried out under cross head displacement speeds of 0.1mm/s (static loading) at room temperature. The experimental equipment was a servo-hydraulic high loading rate tension test machine. Moreover, continuous change in the minimum diameter of necked region or notch root and crack initiation behavior for all types of specimen were observed and recorded by digital microscope of 25 magnifications with facilities of 13mm depth of field. In addition, tensile tests were carried out at cross head displacement speeds at 0.1mm/s (static loading) to 100mm/s (dynamic loading) at root temperature in order to get characteristic of mechanical properties for elastic-plastic, dynamic FE-analysis. The temperature rise was measured by a copper-constant thermocouple which was attached to the central region of a homogeneous round-bar specimens. Furthermore, the same experiment was carried out for base material (HT 80).

The specimens after fracture exhibited typical "cup and cone" type fracture and equiaxed dimples were observed in the T-smooth, T-R2 and T-R1 specimens central region of the fracture surface. In addition, an inflection point in the load/displacement curve appeared just before final ductile failure in T-smooth, T-R2 and T-R1 specimens same as before report. Just after the inflection point, the specimens fractured accompanied by rapid load-decrease. Ductile crack initiation behavior was observed using scanning electrone microscopes (SEM) at longitudinal cross-section in the vicinity of center of a specimen which was unloaded just before and just after the above inflection point. Figure 5 shows an example of a T-R2 specimen, which was just unloaded after the inflection point, as shown in the figure. The microscopic observations suggest that ductile cracking initiates from the growth and coalescence of micro-voids generated between large scale voids in the vicinity of the central of the necking region. Similar results were also observed in both the T-smooth and the T-R1 specimens. According to this observation, the rapid unloading just before final ductile failure occurs due to the appearance of a ductile macro crack in the central region of the specimen and subsequent rapid ductile crack propagation to the specimen surface [6]. Consequently, in the present study, ductile crack initiation from specimen center was defined as the loading level when the inflection point was observed in load P - cross head displacement D_X curve. On the other hand, T-R0.1 specimen was unloaded at certain loading levels before final fracture in order to observe the crack initiation in pre-notch root surface. Fig. 6(b), (c) shows ductile crack initiation behaviors of the T-R0.1 specimen at unloaded level 1 and 2 corresponding to the loading level in true stress-true strain curve, as shown in Fig. 6(a). From these observations, the ductile cracking was not found in the specimen inside, but initiated from the surface of the notch root, in direction of an angle of about 45 degree against tensile axis. In addition, the ductile crack surface about crack length 50mm in level 2 was included the shallow extension dimple in shear mode. As well as, the difference between the group of T-smooth, T-R2 and T-R1 specimens and that of T-R0.1 specimen is observed in

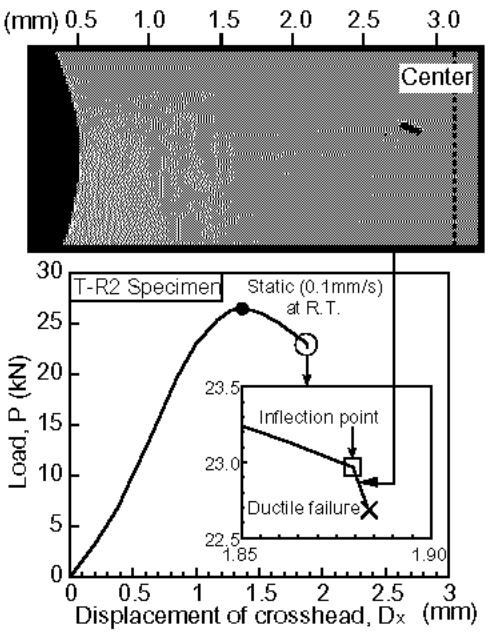

Fig. 5 Ductile crack initiation behavior of *T-R2* specimen under static loading, 0.1mm/s.

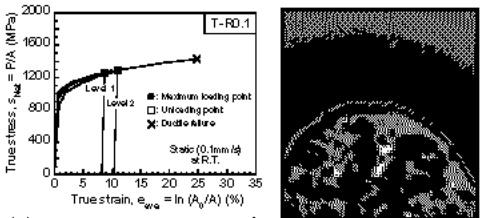

(a) True stress-true stain curves

(b) At level 1

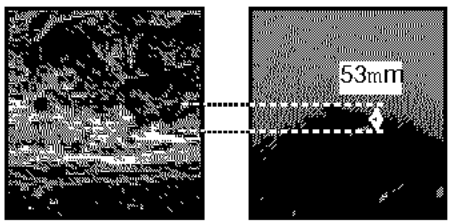

(c) At level 2

Fig. 6 Ductile crack initiation behavior of *T-R0.1* specimen under static loading.

the ductile crack initiation position and the mode of micro-voids growth ; the former is in specimen center with equiaxed mode growth and the letter in specimen surface of pre-notch root with shear mode growth.

3.2 Condition for ductile crack initiation by using FE-analysis

FE-analyses were conducted for the tested round-bar specimens in order to address a stress/strain field of the specimen inside where the ductile crack initiation was confirmed. The FE-models of the present analyses have the same shape and size as the specimens used in experiments. The thermal, elastic-plastic analysis was performed to simulate both the charge in the stress/strain relation and the temperature rise under dynamic loading. The calculation taking to account both heat conduction and elastic-plastic stress analysis, was carried out using the finite element method as implemented in the code ABAQUS version 5.8 [10, 11].

Critical condition for ductile crack initiation of weld metal was estimated using the history of $\bar{e}_p$ and $s_m/\bar{s}$, the relation obtained by FE-analysis as shown in Fig. 7. The critical values of the ductile crack initiation were evaluated by correspondence of true strain $(e_{ave.})_I$ in experiment and FE-analysis. In the case that the ductile crack occurs at specimen surface, the critical strain level is defined when ductile crack length of about 50mm is observed strain level (at level 2 in Fig.6(a)).

The equivalent plastic strain of T-smooth, T-R2 and T-R1, for which ductile crack initiation occurs in the center of specimen, depends largely on the stress triaxiality and decrease with increasing of stress triaxiality $s_m/\bar{s}$. On the other hand, in T-R0.1 specimen that a ductile crack occurred from surface of pre-notch root, the stress triaxiality is almost constant in the history of the $\bar{e}_p$••$s_m/\bar{s}$ relation. The critical value in surface of pre-notch root is not exist on the curve of criterion for ductile crack initiation from center, but show the different lower value comparison with ductile crack initiation from center. From these observations, these results are same as authors result [9], in which get from round bar tensile test. Moreover, it is necessary that the different condition for ductile crack initiation from surface of pre-notch root established for the ductile crack initiation from surface of pre-notch root was different the ductile crack initiation from center.

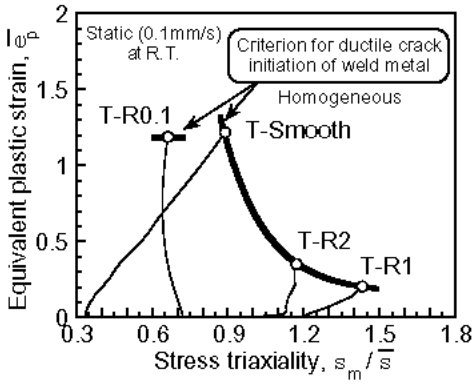

Fig. 7 Criterion for ductile crack initiation from surface and center of specimens in weld metal.

4. Effect of Strength Mismatch on Critical Condition for Ductile Crack Initiation from Pre-notch Root Surface in Bend Specimens

Ductile crack initiation behavior and critical conditions in terms of two-parameter criterion for the specimens with strength mismatch near the notch was discussed by conducting the bending tests and FE-analyses.

4.1 Effect of strength mismatch on ductile crack initi-ation behavior under static and dynamic loading

Figure 8 shows of the relation between load, P and displacement of cross head, D_y and the observation of near the pre-notch root at mid-thickness after unloading for the homogeneous specimen under static loading by SEM (scanning electron microscope). Ductile cracking, which appeared up to the maximum load, occurred from the surface of pre-notch root. The ductile crack of which length is about 50mm occurred along large shear band at loading level 1 and grows large as shown in the micrograph at loading level 2, in direction of an angle of about 45 degree against tensile axials. It has been shown that the ductile crack initiation behaviors would not be influenced by loading mode, as made clear in comparison with those for the tensile specimen T-R0.1.

The effect of strength mismatch on ductile crack initiation behaviors under static and dynamic loading were examined. Figure 9 shows the relation of P-D_y and the SEM observation results near the pre-notch root tip at the middle section of unloading mismatch specimen under dynamic loading. Ductile crack initiation behavior, that is initiation from the pre-notch root surface along shear band in weld metal, is the same as the result of static load. In addition, displacement of cross head, when observed the ductile crack length about 50mm, for homogeneous and mismatch specimen are about 1.7mm and 1.4mm in the dynamic loading. There seem to be no great difference in the ductile crack initiation behaviors between homogeneous and mismatch specimen under both static and dynamic loading.

4.2 Numerical analysis

The stress/strain behaviors in the homogeneous and mismatch specimen were analyzed by coupled heat conduction and elastic-plastic FE-analyses using the same method as those of round-bar specimen in Chapter 3. Figure 10 shows the mesh division used in this analyses. It has same size and shape as bend specimens tested. 8-node isoparametric element is used in this model. Minimum size of element near the pre-notch tip is 0.02• •0.03• •0.5mm. The initial position of the pre-notch root for the model of mismatch specimen was determined by comparing the deformation

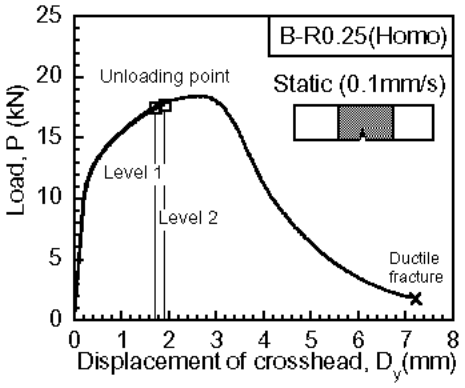

(a) P - D_y curves

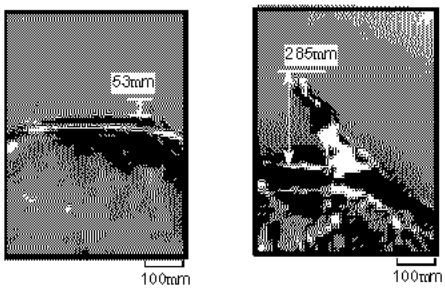

(b) At level 1 (c) At level 2

Fig. 8 Ductile crack initiation behavior of *B-R0.25* (Homogeneous) specimens under static loading, 0.01mm/s.

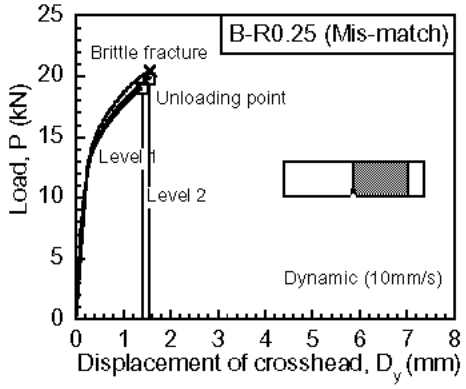

(a) P - D_y curves

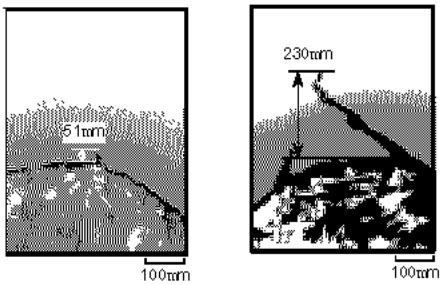

(b) At level 1 (c) At level 2

Fig. 9 Ductile crack initiation behavior of *B-R0.25* (Mis-match) specimens under dynamic loading, 10mm/s.

behavior obtained by FE-analyses and experiments • •the pre-notch root was located at distance 0.24mm from fusion line in the weld metal. Jig used in the actual testing is also modeled as a rigid body, and applied displacement controlling load. The load and applied displacement curves for homogeneous and mismatch specimen under both static and dynamic loading were well consistent with experimental results.

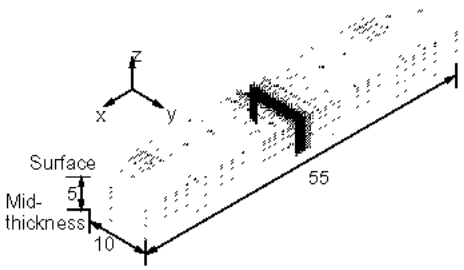

Fig. 10 Mesh division of 3-point bend specimen used for FE-analysis.

4.3 Effect of strength mismatch on critical condition for ductile crack initiation under static and dynamic loading

The critical conditions of ductile crack initiation, which was defined when the crack with length of 50mm from notch root was observed, were estimated using two-parameter, that is equivalent plastic strain $\bar{\varepsilon}_p$ and stress triaxiality $\sigma_m / \bar{\sigma}$. Figure 11 shows the history of $\bar{\varepsilon}_p$•• $\sigma_m / \bar{\sigma}$ the relation at ductile crack initiation for surface of pre-notch root in maximum strain element for homogeneous and strength mismatch bend specimens under static loading. There is no effect of strength mismatch in the history of $\bar{\varepsilon}_p$••$\sigma_m / \bar{\sigma}$ the relation, and the critical value for strength mismatch specimen has slightly lower value than that for homogeneous specimen, however, they are almost same. In addition, these results ware same as round bar tensile test result as surface ductile crack initiation type. Furthermore, in comparison with the criterion obtained with tensile specimens, they are not on the critical curves for the specimens with ductile cracking from center but on the critical value for T-R0.1 specimen with surface crack initiation. Also in the case of dynamic loading, the similar results were given and no effect of strength mismatch on critical condition for ductile cracking from the surface of pre-notch root was observed as presented in Fig. 12. Consequently, it was demonstrated that two-parameter criterion would be applicable to the ductile cracking from surface of pre-notch root in strength mismatch specimen under both static and dynamic loading by conducting the coupled heat conduction and elastic-plastic FE-analyses. And they would be in accordance with constant plastic strain condition as a surface cracking type of specimen.

5. Conclusions

The criterion for ductile crack initiation from notch root of bend specimens with strength mismatch under static, criterion. It was demonstrated that two-parameter criterion would be applicable to the ductile cracking from notch

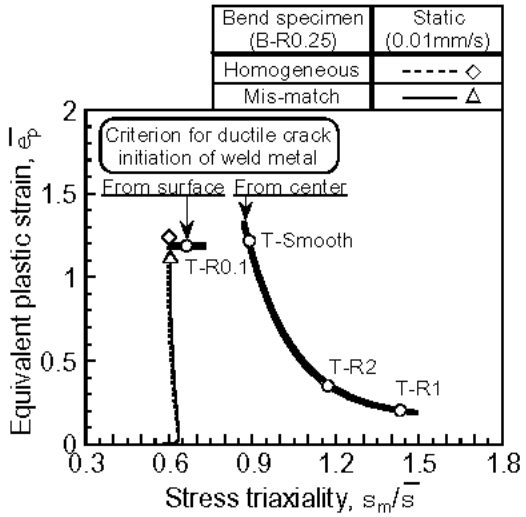

Fig.11 Condition for ductile cracking using two parameters, $\bar{\varepsilon}_p$ and $s_m/\bar{s}$, for homogeneous and mis-match specimens under static loading.

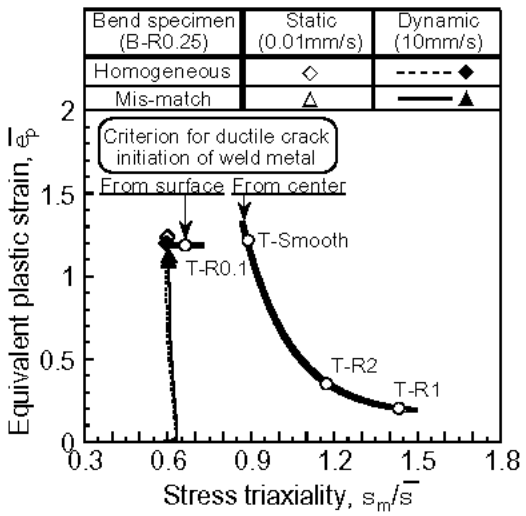

Fig. 12 Condition for ductile cracking using two parameters, $\bar{\varepsilon}_p$ and $s_m/\bar{s}$, for homogeneous and mis-match specimens under dynamic loading.

root in strength mismatch specimen also in the case of dynamic loading by conducting the coupled heat conduction and elastic-plastic FE-analyses employed in this study. Moreover, they would be in accordance with constant plastic strain condition as a surface cracking type of specimen under both static and dynamic loading.

These results implies that, if the critical condition for ductile crack initiation for the steel will be given by conducting tensile tests and FE-analyses for round-bar specimens, the critical applied load with respect to ductile cracking of steel structures with strength mismatch under different condition of loading mode and loading rate can be evaluated by carrying out only this coupled thermal elastic-plastic FE-analysis by applying the two-parameter criterion.

References

[1] AIJ : *Steel Committee of Kinki Branch*, (1995) .
[2] M. Toyoda : *Welding Journal*, 74 (1995), p. 31s.
[3] K. Okashita, R. Ohminami, K. Michiba, A. Yamamoto, M. Tomimatsu, T, Tanji, C. Miki: *Journals of the Japan Society of Civil Engineers*, 591(1998), I-43, p.243s.
[4] APD Committee: *The Japan Welding Engineering Society*, JWES-IS-0002 (2000).
[5] H. Shimanuki and Y. Hagiwara : *Preprints of the National Meeting of J.W.S.*, (1994), p. 412s.
[6] H. Shimanuki, H. Furuya, T. Inoue, Y. Hagiwara and M. Toyoda : *Journal of the Society of Naval Architects of Japan*, 186 (1999), p. 475s.
[7] M. Toyoda, M. Ohata, N. Ayukawa, G. Ohwaki, Y. Ueda, I. Takeuchi: *Proc. 3rd Int. Pipeline Technology Conf.*, Brugge, Belgium, 2(2000), p.87-102.
[8] O. Yasuda, M. Hirono, M. Yokota, M. Ohata, M. Toyoda: *Journal of Constructional Steel*, 8(2000), p. 425s.
[9] G.B. An, S. Yoshida, Z. Praunseis, M. Ohata and M. Toyoda : *Journal of the Society of Naval Architects of Japan*, 189 (2001), p. 375s.
[10] M. Toyoda, M. Mochizuki, T. Ohmura, and G.B. An : *Proceedings of the International Seminar on Numerical Analysis in Solid and Fluid Dynamics in 1999*, Suita, Japan, (1999), p. 217s
[11] Hibbit, Karlsson, Sorensen, Inc: ABAQUS/Standard User's Manuals Ver. 5.8, 1 to 3(1998).